Westfälische Wilhelms-Universität Münster

Center for Nonlinear Science

Münsteranian Torturials on Nonlinear Science

edited by Uwe Thiele, Oliver Kamps, Svetlana Gurevich

# Continuation

## DROP : Steady drop and film states on a horizontal homogeneous substrate

Uwe Thiele

with the support of

Christian Schelte, Frank Ehebrecht

Version 1, Feb 2015

For updates of this text and the accompanying programme files see
www.uni-muenster.de/CeNoS/Lehre/Tutorials/auto.html

# 1 drop : Steady drop and film states on a horizontal homogeneous substrate

The tutorial DROP explores an equation for steady drop-and-hole solutions derived from the dimensionless thin film (or lubrication) equation. You will calculate steady solution of the equation by continuation in a number of different control parameters (domain size, mean height).

## 1.1 Model

This demo illustrates the calculation of steady drop and hole solutions of the dimensionless thin film (or long-wave) equation

$$\partial_t h \;=\; -\partial_x \left\{Q(h)\,\partial_x \left[\partial_{xx}h - \partial_h f(h)\right]\right\} \tag{1.1}$$

where $Q(h) = h^3$ is the mobility factor (not relevant for steady states). For background information see [1, 2, 3, 4]. The term in square brackets represents the negative of a pressure that consists of the Laplace (or curvature) pressure $-\partial_{xx}h$ and an additional contribution $\partial_h f(h)$ written as the derivative of a local free energy $f(h)$. The Laplace pressure is the pressure difference across a curved interface caused by its surface tension. If $R_1$ and $R_2$ are the principal radii of curvature the pressure jump is proportional to $\frac{1}{R_1} + \frac{1}{R_2}$. Here, only the curvature of the free surface of the drop gives a contribution, which is in long-wave approximation approximatly the second spacial derivative of the height profile.

The local free energy has a particular form for each studied problem. For specific examples see [5, 6, 7, 8, 9, 10]. In the demo we use a simple Derjaguin (or disjoining/conjoining) pressure $\Pi(h) = -\partial_h f(h)$ that describes wettability for a partially wetting liquid (see reviews [11, 12, 13]). In particular, we employ a combination of two inverse power laws in $h$ [7, 14].

$$\partial_h f(h) = -\Pi(h) = \frac{1}{h^3} - \frac{1}{h^6}. \tag{1.2}$$

To study steady solutions, i.e., resting droplets or films, we set $\partial_t h = 0$ and integrate Eq. (1.1) twice (this is possible as the first integration constant, the flux $C_0$, is zero for systems without through-flow [3], then one may divide by $Q(h) \neq 0$ and the second time.

One obtains

$$0 \;=\; \partial_{xx}h(x) \;-\; \partial_h f(h) \;+\; C_1. \tag{1.3}$$

The constant $C_1$ accounts for external conditions like chemical potential, vapor pressure or mass conservation. Here we consider the latter case where $C_1$ takes the role of a Lagrange multiplier for mass conservation. To use the continuation toolbox auto07p [15], we first write (1.3) as a system of first-order autonomous ordinary differential equations on the interval $[0, 1]$. Therefore, we introduce the variables $u_1 = h - h_0$ and $u_2 = dh/dx$, and obtain from equation (1.3) the 2d dynamical system ($\mathrm{NDIM} = 2$)

$$\begin{aligned} \dot{u}_1 &= L u_2 \\ \dot{u}_2 &= L\,[f'(h_0 + u_1) \;-\; C_1]. \end{aligned} \tag{1.4}$$

where $L$ is the physical domain size, and dots and primes denote derivatives with respect to $\xi \equiv x/L$ and $h$, respectively. The advantage of the used form is that the fields $u_1(\xi)$ and $u_2(\xi)$

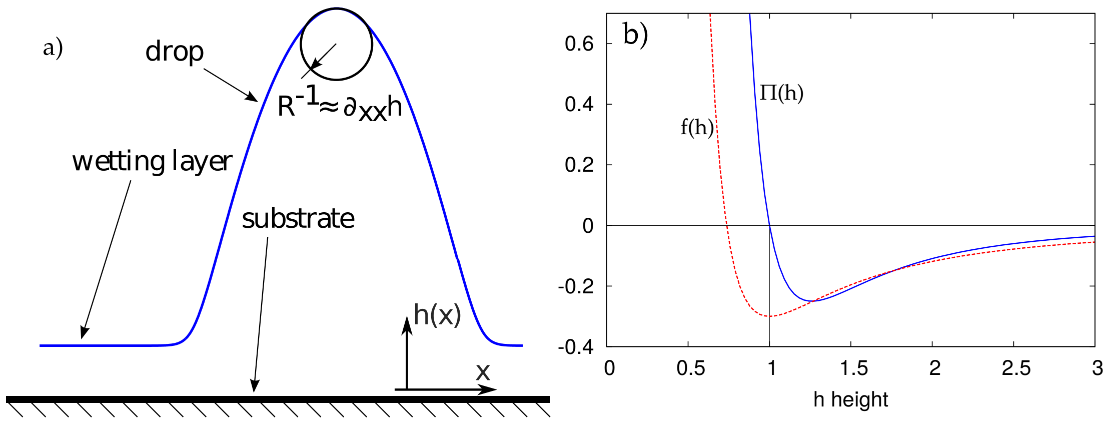


**Figure 1.1:** Panel (a) provides a sketch of the geometry employed in the demo `drop`. It shows a small droplet that coexists with an ultrathin wetting layer (precursor film) in a situation with laterally periodic boundary conditions, as introduced in Eq. (1.6). Note that the radius of curvature can be both positiv and negative and competes with the Derjaguin pressure $\Pi(h)$. Panel (b) gives typical functional dependencies on $h$ of the Derjagin pressure and the local free energy $f(h)$.

correspond to the correctly scaled physical fields $h(L\xi)$ and $\partial_x h(L\xi)$. We use periodic boundary conditions for $u_1$ and $u_2$ ($\mathrm{NBC} = 2$) that take the form

$$u_1(0) = u_1(1), \tag{1.5}$$
$$u_2(0) = u_2(1), \tag{1.6}$$

and integral conditions for mass conservation and computational pinning (to break the translational symmetry that the solutions have on the considered homogeneous substrate) ($\mathrm{NINT} = 2$). The integral condition for mass conservation takes the form

$$\int_0^1 u_1 \,\mathrm{d}\xi = 0. \tag{1.7}$$

As starting solution we use a small amplitude harmonic modulation of wavelength $L_c = 2\pi/k_c$ where $k_c = \sqrt{-f''(h_0)}$ is the critical wavenumber for the linear instability of a flat film of thickness $h_0$. This results in $C_1 = f'(h_0)$ as starting value for $C_1$.

The number of free (continuation) parameters is given by $\mathrm{NCONT} = \mathrm{NBC}+\mathrm{NINT}-\mathrm{NDIM}+1$ and is here equal to 3.

There is a further complication as Eq. (1.3) corresponds to a conservative dynamical system (not a dissipative one). To deal with this we employ an 'unfolding parameter' $\epsilon$ that transforms the conservative in a 'virtual' dissipative system (with the same solutions). Different formulations are possible. Here we use:

$$\begin{aligned} \dot{u}_1 &= Lu_2 - \epsilon[f'(\bar{h}+u_1) \;-\; C_1] \\ \dot{u}_2 &= L\,[f'(\bar{h}+u_1) \;-\; C_1]. \end{aligned} \tag{1.8}$$

The technique is mentioned in the auto07p [15] demo 'r3b' and further explained in Refs. [16, 17, 18]. It corresponds to the introduction of an unfolding term that embeds the conservative system into a one-parameter family of dissipative systems. Thereby the unfolding parameter $\epsilon$ creates a one-parameter family of periodic solutions. Periodic solutions only exist for $\epsilon = 0$.

## 1.2 Runs:

| Python interface command line | Terminal command line |
|---|---|
| *auto* | |
| **run 1:** Determine steady solutions as a function of domain size $L$, starting at the critical $L_c$ with a small amplitude sinusoidal solution. Mean thickness $h_0 = 3$ is fixed. One finds that the primary bifurcation is subcritical, and that the branch turns towards larger $L$ at a saddle-node bifurcation at some $L_{\text{sn}} < L_c$. Compute the branch of periodic solutions for $h_0 = 3$ continued in $L$ (PAR(5)) up to $L = 100$.<br>**Remaining true continuation parameters:** $C_1$ (PAR(6)) and $\epsilon$ (PAR(2));<br>**Other output:** amplitude of $h$ (PAR(7)), maximal slope of $h$. i.e., the mesoscopic contact angle $\theta_{\text{mes}}$ (PAR(46))<br>**Parameter:** IPS= 4, ISP= 0, ISW= 1, ICP= $[5, 6, 2, 7, 46]$,<br>Start data from function $stpnt$ (IRS= 0)<br>save output-files as `b.d1, s.d1, d.d1` | |
| *r1 = run(e = 'drop', c = 'drop.1', sv = 'd1')* | *@@R drop 1*<br>*@sv d1* |
| **run 11:** Restart at domain size $L = 100$, change mean thickness $h_0$.<br>Continued in mean thickness $h_0$ (PAR(1)) for fixed domain size $L$. Stop at $h_0 = 10$<br>**Remaining true continuation parameters:** $C_1$ (PAR(6)) and $\epsilon$ (PAR(2))<br>**Other output:** as in run 1<br>**Parameters:** IPS= 4, ISP= 0, ISW= 1, ICP= $[1, 6, 2, 7, 46]$,<br>Start at final result of run 1: IRS= 7<br>save output-files as `b.d11, s.d11, d.d11` | |
| *r11 = run(r1, e = 'drop', c = 'drop.11', sv = 'd11')* | *@@R drop 11 d1*<br>*@sv d11* |
| **run 2:** Same as run 1 but continuing to large drops $L = 10^5$.<br>save output-files as `b.d2, s.d2, d.d2` | |
| *r2 = run(e = 'drop', c = 'drop.2', sv = 'd2')* | *@@R drop 2*<br>*@sv d2* |
| Plot the results. | |
| *plot('d1')*<br>*plot('d11')*<br>*plot('d2')* | *@pp d1*<br>*@pp d11*<br>*@pp d2* |
| *clean()* | *@cl* |

**Table 1.1:** Commands for running demo `drop`.

## 1.3 Remarks:

- In thermodynamic context, the constant $C_1$ corresponds to the negative of the chemical potential.
- The *.f90 file provides another integral condition that is not used in the demo. If used it allows for a determination of the energy of the obtained steady state solutions.
- Beside the NCONT true continuation parameters that have to be given as ICP in the c.*

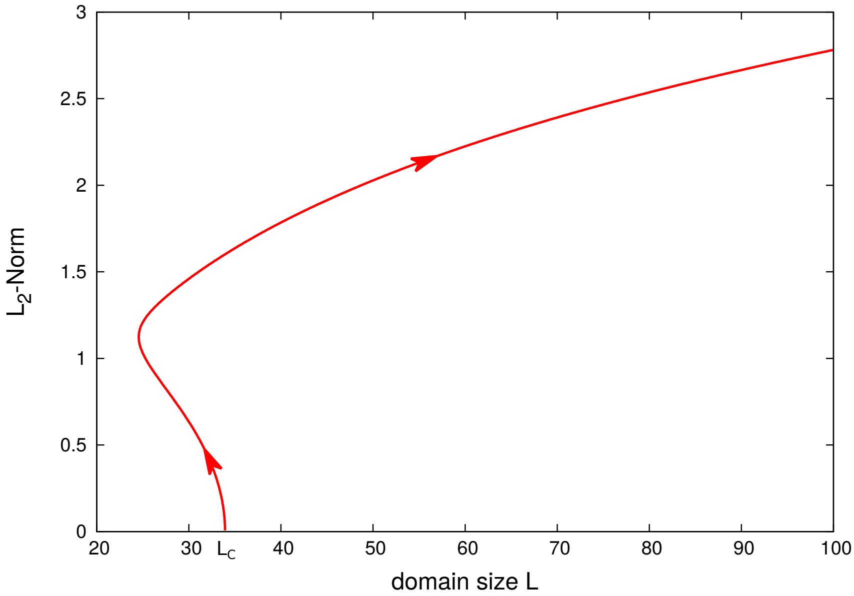


**Figure 1.2:** An illustration for run 1 of demo `drop` is given. The $L_2$-norm of steady solutions is shown in dependence of the principal continuation parameter domain size $L$ (par(5)) for mean film thickness $h_0 = 3.0$. The arrow indicates the direction of the path continuation.

parameter file, one may list other output parameters as defined in the subroutine PVLS in the *.f90 file.

- Screen output and command line commands are provided in README file.

## 1.4 Tasks:

After running the examples, you should try to implement your own adaptations, e.g.:

1. Redo run 1 for other values of $h_0$, e.g., 1.27, 1.5, 2.5, 5.0, 10.0. What do you observe?
2. Redo run 11 allowing the code to go beyond $h_0 = 10$. What do you observe?
3. Try to run a continuation with fixed $C_1$ (you need to 'set free' another parameter). Compare your results with [4].
4. Activate the additional integral condition to measure the energy

$$E = \int_L \left(\frac{u_2^2}{2} + f(h) - f(h_0)\right) \mathrm{d}\xi \tag{1.9}$$

of the solutions.

5. Replace the used Derjaguin pressure by a different one that you get from the literature. ([8], [19] or [5])

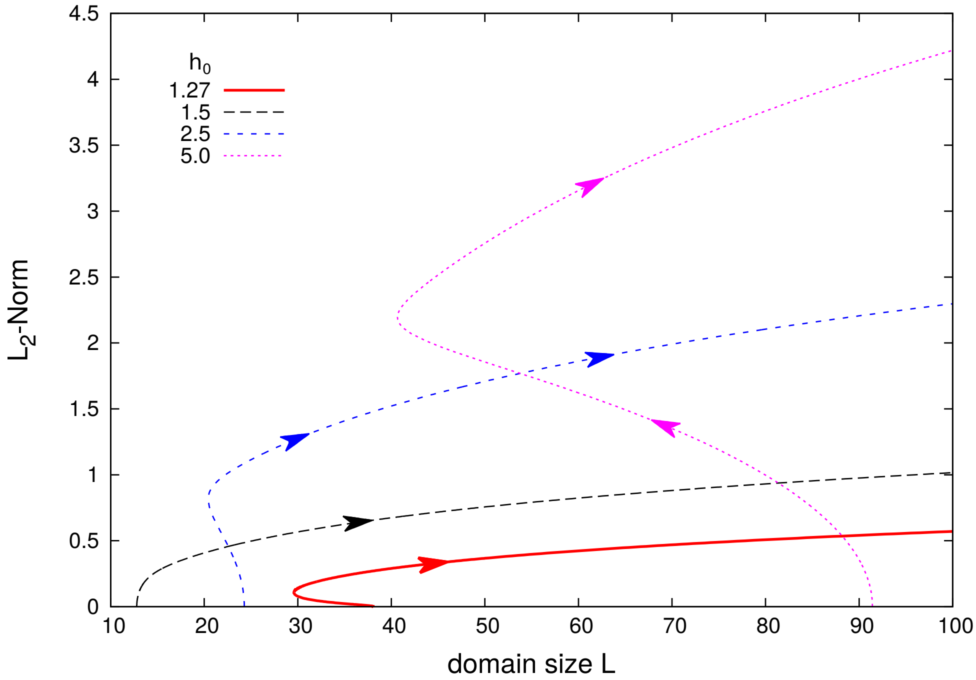


**Figure 1.3:** An illustration for task 1 of demo `drop` is given. The $L_2$-norm of steady solutions is shown in dependence of the principal continuation parameter domain size $L$ (par(5)) for various fixed mean film thicknesses as given in the legend.

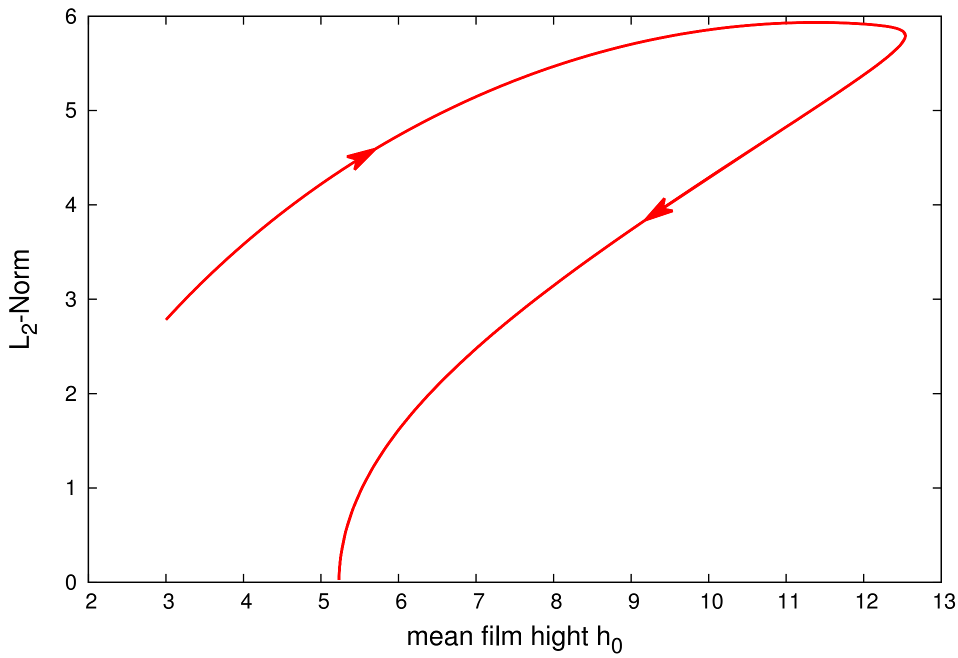


**Figure 1.4:** An illustration for task 2 of demo `drop` is given. The $L_2$-norm of steady solutions is shown in dependence of the principal continuation parameter mean film height $h_0$ (par(1)) for fixed domain size $L = 100$. The drop size increases with $h_0$ up to $h_0 \approx 12.5$ where a saddle-node bifurcation occurs (the drop fills the entire domain). The lower branch corresponds to unstable hole (nucleation) solutions. The arrow indicates the direction of the path continuation.

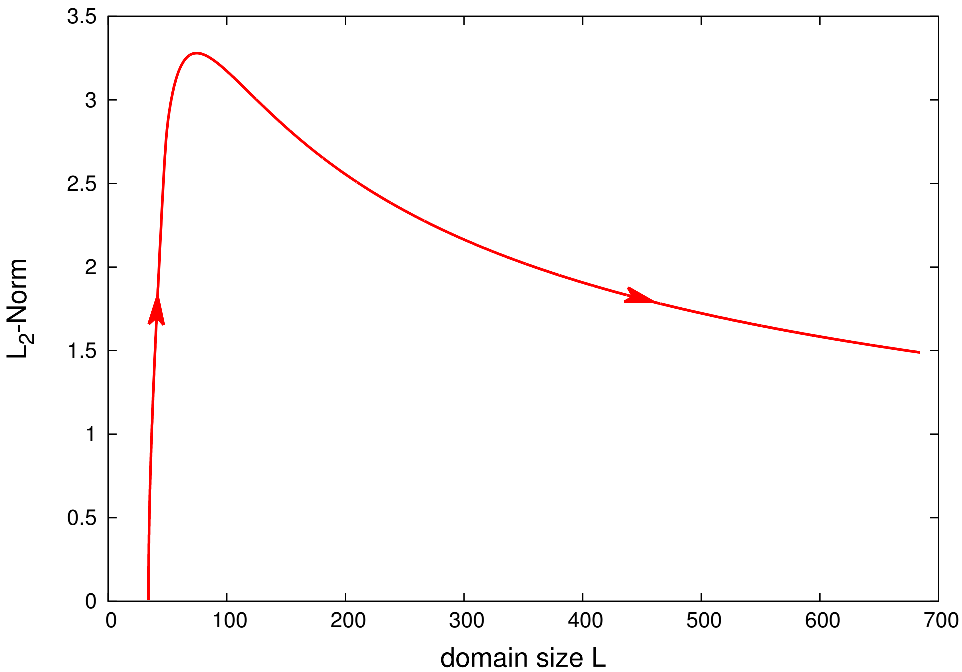


**Figure 1.5:** An illustration for task 3 of demo `drop` is given. The $L_2$-norm of steady solutions is shown in dependence of the principal continuation domain size $L$ (par(5)) for fixed chemical potential $C_1 = f(h = 0)$ (par(6)).

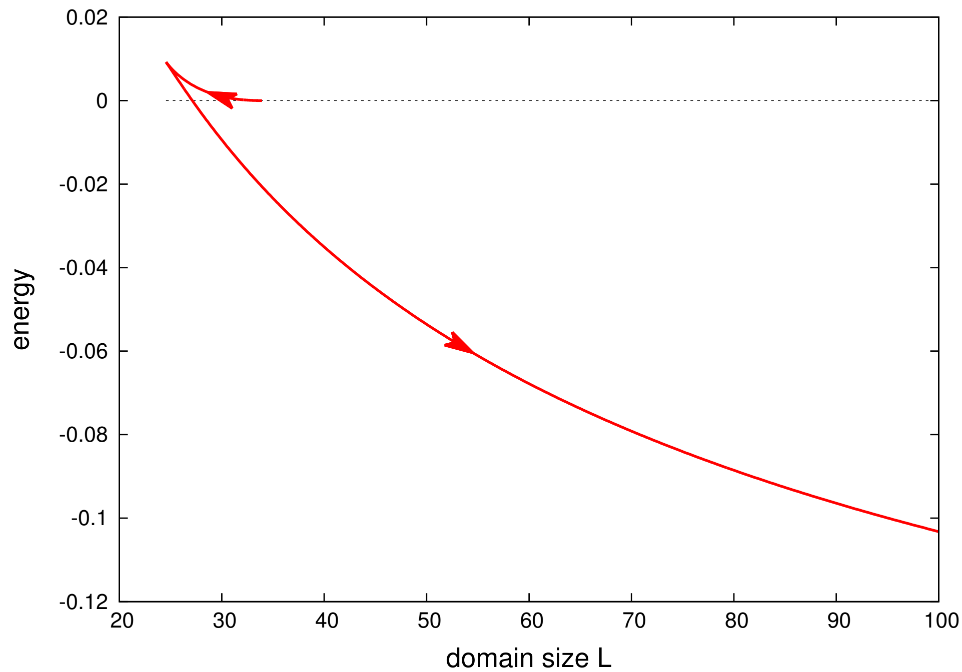


**Figure 1.6:** An illustration for task 4 of demo `drop` is given. The energy (1.9) of steady solutions is shown in dependence of the principal continuation parameter domain size $L$ (par(5)) for fixed mean film thickness $h_o = 3.0$.

## References

[1] V. S. Mitlin. "Dewetting of solid surface: Analogy with spinodal decomposition". In: *J. Colloid Interface Sci.* 156 (1993), pp. 491–497. DOI: `10.1006/jcis.1993.1142`.

[2] A. Oron, S. H. Davis, and S. G. Bankoff. "Long-scale evolution of thin liquid films". In: *Rev. Mod. Phys.* 69 (1997), pp. 931–980. DOI: 10.1103/RevModPhys.69.931.

[3] U. Thiele. "Structure formation in thin liquid films". In: *Thin Films of Soft Matter*. Ed. by S. Kalliadasis and U. Thiele. Wien: Springer, 2007, pp. 25–93. DOI: 10.1007/978-3-211-69808-2_2.

[4] U. Thiele. "Thin film evolution equations from (evaporating) dewetting liquid layers to epitaxial growth". In: *J. Phys.: Condens. Matter* 22 (2010), p. 084019. DOI: 10.1088/0953-8984/22/8/084019.

[5] A. Sharma. "Equilibrium contact angles and film thicknesses in the apolar and polar systems: Role of intermolecular interactionsin coexistence of drops with thin films". In: *Langmuir* 9 (1993), p. 3580.

[6] G. F. Teletzke, H. T. Davis, and L. E. Scriven. "Wetting hydrodynamics". In: *Rev. Phys. Appl. (Paris)* 23 (1988), pp. 989–1007. DOI: 10.1051/rphysap:01988002306098900.

[7] L. M. Pismen. "Nonlocal diffuse interface theory of thin films and the moving contact line". In: *Phys. Rev. E* 64 (2001), p. 021603. DOI: 10.1103/PhysRevE.64.021603.

[8] U. Thiele, M. G. Velarde, and K. Neuffer. "Dewetting: Film rupture by nucleation in the spinodal regime". In: *Phys. Rev. Lett.* 87 (2001), p. 016104. DOI: 10.1103/PhysRevLett.87.016104.

[9] U. Thiele et al. "Film rupture in the diffuse interface model coupled to hydrodynamics". In: *Phys. Rev. E* 64 (2001), p. 031602. DOI: 10.1103/PhysRevE.64.031602.

[10] U. Thiele and E. Knobloch. "Thin liquid films on a slightly inclined heated plate". In: *Physica D* 190 (2004), pp. 213–248.

[11] V. M. Starov and M. G. Velarde. "Surface forces and wetting phenomena". In: *J. Phys.-Condens. Matter* 21 (2009), p. 464121. DOI: 10.1088/0953-8984/21/46/464121.

[12] P.-G. de Gennes. "Wetting: Statics and dynamics". In: *Rev. Mod. Phys.* 57 (1985), pp. 827–863. DOI: 10.1103/RevModPhys.57.827.

[13] D. Bonn et al. "Wetting and spreading". In: *Rev. Mod. Phys.* 81 (2009), pp. 739–805. DOI: 10.1103/RevModPhys.81.739.

[14] L. M. Pismen and U. Thiele. "Asymptotic theory for a moving droplet driven by a wettability gradient". In: *Phys. Fluids* 18 (2006), p. 042104. DOI: 10.1063/1.2191015.

[15] E.J. Doedel and B.E. Oldeman. *AUTO-07P :Continuation and bifurcation software for ordinary differential equations*. http://www.dam.brown.edu/people/sandsted/auto/auto07p.pdf. 2012.

[16] E. J. Doedel et al. "Computation of periodic solutions of conservative systems with application to the 3-body problem". In: *Int. J. Bifurcation Chaos* 13 (2003), pp. 1353–1381. DOI: 10.1142/S0218127403007291.

[17] FJ Munoz-Almaraz et al. "Continuation of periodic orbits in conservative and Hamiltonian systems". In: *Physica D* 181 (2003), pp. 1–38. DOI: 10.1016/S0167-2789(03)00097-6.

[18] FJ Munoz-Almaraz et al. "Continuation of normal doubly symmetric orbits in conservative reversible systems". In: *Celest. Mech. Dyn. Astron.* 97 (2007), pp. 17–47. DOI: 10.1007/s10569-006-9048-3.

[19] A. Sharma. "Relationship of thin film stability and morphology to macroscopic parameters of wetting in the apolar and polarsystems". In: *Langmuir* 9 (1993), pp. 861–869. DOI: 10.1021/la00027a042.